1521-0103/376/1/1–11$35.00
THE JOURNAL OF PHARMACOLOGY AND EXPERIMENTAL THERAPEUTICS

https://doi.org/10.1124/jpet.120.000163
J Pharmacol Exp Ther 376:1–11, January 2021

Mechanism of Diuresis and Natriuresis by Cannabinoids: Evidence for Inhibition of Na^+-K^+-ATPase in Mouse Kidney Thick Ascending Limb Tubules[S]

Joseph K. Ritter, Ashfaq Ahmad, Shobha Mummalaneni, Zdravka Daneva, Sara K. Dempsey, Ningjun Li, Pin-Lan Li, and Vijay Lyall

Departments of Pharmacology and Toxicology (J.K.R., A.A., Z.D., S.K.D., N.L., P.-L.L.) and Physiology and Biophysics (S.M., V.L.), Virginia Commonwealth University, Richmond, Virginia

Received June 11, 2020; accepted October 6, 2020

ABSTRACT

The endocannabinoid, anandamide (AEA), stimulates cannabinoid receptors (CBRs) and is enriched in the kidney, especially the renal medulla. AEA infused into the renal outer medulla of mice stimulates urine flow rate and salt excretion. Here we show that these effects are blocked by the CBR type 1 (CB1) inverse agonist, rimonabant. Immunohistochemical analysis demonstrated the presence of CB1 in thick ascending limb (TAL) tubules. Western immunoblotting demonstrated the presence of CB1 (52 kDa) in the cortex and outer medulla of mouse kidney. The effect of direct [CP55940 (CP) or AEA] or indirect [fatty acyl amide hydrolase (FAAH) inhibitor, PF3845 (PF)] cannabinoidimetics on Na^+ transport in isolated mouse TAL tubules was studied using the Na^+-sensitive dye, SBFI-AM. Switching from 0 Na^+ solution to control Ringer's solution (CR) rapidly increased TAL cell $[Na^+]_i$. Addition of CP to CR produced a further elevation, similar in magnitude to that of ouabain, a Na^+-K^+-ATPase inhibitor. This $[Na^+]_i$-elevating effect of CP was time-dependent, required the presence of Na^+ in the bathing solution, and was insensitive to Na^+-K^+-$2Cl^-$ cotransporter inhibition. Addition of PF to CR elevated $[Na^+]_i$ in FAAH wild-type but not FAAH knockout (KO) TALs, whereas the additions of CP and AEA to PF-treated FAAH KO TALs increased $[Na^+]_i$. An interaction between cannabinoidimetics and ouabain (Ou) was observed. Ou produced less increase in $[Na^+]_i$ after cannabinoidimetic treatment, whereas cannabinoidimetics had less effect after Ou treatment. It is concluded that cannabinoidimetics, including CP and AEA, inhibit Na^+ transport in TALs by inhibiting Na^+ exit via Na^+-K^+-ATPase.

SIGNIFICANCE STATEMENT

Cannabinoids including endocannabinoids induce renal urine and salt excretion and are proposed to play a physiological role in the regulation of blood pressure. Our data suggest that the mechanism of the cannabinoids involves inhibition of the sodium pump, Na^+-K^+-ATPase, in thick ascending limb cells and, likely, other proximal and distal tubular segments of the kidney nephron.

Introduction

Marijuana, the most commonly used illicit psychotropic drug in the United States, has the four primary pharmacologic effects associated with cannabinoids: decreased locomotor activity, hypothermia, cataleptic effects, and analgesia (Little et al., 1988). These cannabinoid receptor (CBR)–mediated effects are recapitulated by (−)-*trans*-Δ^9-tetrahydrocannabinol (THC), the main psychoactive constituent of marijuana and a nonselective partial agonist at the cannabinoid receptor type 1 (CB1) and type 2 receptors. In addition, both marijuana and THC elicit profound effects on the heart and kidneys, decreasing heart rate and blood pressure (Vollmer et al., 1974; Lake et al., 1997; Benowitz and Jones, 1975) and increasing urine production (Sofia et al., 1977; Chopda et al., 2013). In kidneys, the effect of THC on urine and Na^+ output in rats was comparable to the thiazide diuretic, hydrochlorothiazide (Sofia et al., 1977). More recently, various direct-acting CB1 agonists, including THC, WIN55212-2, AM2389, and AM4054 were shown to elicit diuretic effects in rats with ED50 values comparable to those for hypothermia. The effect of at least one of these agonists, AM4054, was antagonized by pretreatment with rimonabant, a CB1-selective inverse agonist (Chopda et al., 2013; Paronis et al., 2013). Similar effects of CB1 agonists were described in mice with evidence of blockade by

This work was supported by National Institutes of Health National Institute of Digestive and Kidney Disorders [Grant DK102539] and National Institute on Drug Abuse [Grants P30DA033934 and T32DA007027].
https://doi.org/10.1124/jpet.120.000163.
[S] This article has supplemental material available at jpet.aspetjournals.org.

ABBREVIATIONS: AEA, anandamide; Bu, bumetanide; CB1, cannabinoid receptor type 1; CBR, cannabinoid receptor; CP, CP55940; CR, control Ringer's solution; FAAH, fatty acyl amide hydrolase; FIR, fluorescence intensity ratio; HBSS, Hanks' balanced salt solution; KO, knockout; MAP, mean arterial pressure; mTAL, medullary thick ascending limb; 0 NaR, 0 Na^+ Ringer's solution; NKCC2, Na^+-K^+-$2Cl^-$ cotransporter; Ou, ouabain; PF, PF3845; RIM, rimonabant; ROI, region of interest; SBFI-AM, 1,3-benzenedicarboxylic acid, 4,4′-[1,4,10-trioxa-7,13-diazacyclo-pentadecane-7,13-diylbis(5-methoxy-6,12-benzo-furandiyl]-bistetrakis(acetyloxy) methyl ester; TAL, thick ascending limb of Henle's loop; THC, tetrahydrocannabinol; UNa, urinary sodium excretion rate; URB, URB597; WT, wild type.

CB1 blockers (Chopda et al., 2013; Paronis et al., 2013). Work in our laboratory has shown that intramedullary infusion of the endocannabinoid, N-arachidonoylethanolamide (AEA), stimulates diuresis and salt excretion in mice, suggesting that at least one cellular target of AEA lies in the renal medulla. This hypothesis is supported by the observation that the renal medulla is enriched in AEA relative to the cortex (Ritter et al., 2012). In addition, intramedullary infusions of a structural derivative of AEA and direct CB1 agonist, methanandamide, as well as indirect cannabinoidimetics that elevate AEA by inhibiting its hydrolysis by fatty acid amyl hydrolase (FAAH), also stimulate diuresis and natriuresis (Ahmad et al., 2017, 2018).

The mechanism of CB1-mediated diuresis in kidney is partially understood. Silva et al. studied oxygen consumption in medullary thick ascending limb (mTAL) tubules of rat kidney and found that AEA inhibited oxygen consumption by a mechanism sensitive to inhibition of Na^+ entry into thick ascending limb (TAL) cells (Silva et al., 2013). This effect was also evident with WIN55212-2, a synthetic nonselective CBR agonist, and was inhibited by rimonabant (10 μM), suggesting that CB1 activation inhibits Na^+ transport in TAL cells. In addition to its effects on excretory functions of the kidney, AEA is present in renal endothelial cells and promotes vasorelaxation of afferent arterioles of juxtaglomerular nephrons. These observations suggest that diuresis by AEA may also occur through effects on renomedullary hemodynamics (Deutsch et al., 1997).

The objective of this study was to determine the contribution of CBR in the in vivo mechanism of diuresis and increased salt excretion in the renal medulla by AEA. We evaluated the effect of pretreatment with the CB1 inverse agonist, rimonabant, on the acute response to intramedullary AEA infusion. Next, we investigated the effect of AEA and direct and indirect CBR agonists on Na^+ transport in TAL tubules isolated from the outer medulla of mouse kidneys and loaded with the Na^+-sensitive dye, 1,3-benzenedicarboxylic acid, 4,4′-[1,4,10-trioxa-7,13-diazacyclo-pentadecane-7,13-diylbis(5-methoxy-6,12-benzo-furandiyl]-bistetrakis(acetyloxy) methyl ester (SBFI-AM). Their identity as TAL tubules was confirmed by demonstrating their sensitivity to bumetanide (Bu), one of the prototype Na^+-K^+-$2Cl^-$ cotransporter (NKCC2) inhibitors used therapeutically. Combined with data from immunohistochemical and Western blot analyses of CB1 in mouse kidney, our results suggest that cannabinoidimetics inhibit Na^+ transport through TAL cells by a CB receptor-dependent mechanism involving inhibition of sodium transport by Na^+-K^+-ATPase.

Materials and Methods

Materials. Gibco Collagenase type IV from *Clostridium histolyticum* was cell culture grade from Thermo Fisher Scientific (Carlsbad, CA). AEA, rimonabant, (+)-CP55940 (CP), URB597 (URB), and SBFI-AM were purchased from Cayman Chemical (Ann Arbor, MI). PF3845 (PF) was from APExBIO (Houston, TX). Oubain (Ou) was purchased from Sigma-Aldrich (St. Louis, MO). All other reagents for in vivo or in vitro use (cell culture) were of the highest grade available.

Animals. This study used 10 wild-type and three knockout mice (2–4 months old, mainly male) from a colony of FAAH knockout mice maintained in the Transgenic/Knock-Out Mouse Shared Resource at Virginia Commonwealth University. The mice used in experiments weighed 25 ± 5 g and were housed four to five per cage in a temperature- (20–22°C) and humidity-controlled (50%–55%) facility with a 12/12 hours light/dark cycle and ad libitum food and water. All animal protocols were approved by the Institutional Animal Care and Use Committee of Virginia Commonwealth University and were in concordance with the National Institutes of Health Guide for the Care and Use of Laboratory Animals.

Acute Renal Function Assay. The acute renal function test was performed as described previously (Ritter et al., 2012; Ahmad et al., 2017, 2018). Briefly, mice were anesthetized with Inactin (thiobutabarbital) and ketamine, tracheotomized with PE-60 polyethylene tubing, cannulated in the left carotid artery with a section of heparin/saline-filled pulled PE-10 tubing attached to a pressure transducer for blood pressure monitoring (Windaq; DATAQ Instruments, Akron, OH), cannulated in the right jugular vein for infusion of 0.9% saline for the duration of the experiment (1 ml/h per 100 g body weight) to maintain fluid volume and hematocrit concentration. The left ureter was ligated and cut on the kidney side to allow urine produced by the left kidney to exit freely into the abdominal cavity and to prevent urine backflow from the bladder. The right kidney was cannulated with the tip of a pulled PE-10 catheter implanted to a depth of 2.5 mm vertically from the dorsal surface and anchored to the kidney capsule using VetBond tissue adhesive (3M Animal Care Products, St. Paul, MN). The infusion solution contained phosphate-buffered saline (205 mM NaCl, 40.5 mM Na_2HPO_4, and 9.5 mM NaH_2PO_4 (pH 7.4, 610 mOsM) and 10% ethanol at a rate of 2 μl/min. To measure urine flow rate, the bladder was cannulated with a 2.5 cm cut length of PE-50 tubing, and urine was collected in timed 10-minute intervals into preweighed tubes for gravimetric determination of urine volume. All urinary parameters were calculated on a per gram kidney weight basis. After a 1-hour equilibration period to establish a stable baseline, urine was collected for two 10-minute control periods designated C1 and C2. AEA was administered into the renal medulla in the infusion solution at rates of 15, 30, and 60 nmol/min per kilogram for 30-minute at each dose. The mean value between 10 and 30 minutes was calculated and used as the average at each dose level. The effect of rimonabant on the AEA response was tested by administering an i.p. bolus dose (3 mg/kg) 30-minute prior to the start of AEA infusion (Wise et al., 2007). Sham control mice received the intravenous vehicle (0.9% saline) and intramedullary vehicle solutions for the entire experimental duration. At the termination of the experiment, mice were euthanized by collection of blood through the carotid artery catheter into a heparinized tube. Plasma was collected by centrifugation for 3 minutes at 3000 rpm in a microcentrifuge, and the right kidney was removed and weighed and stored along with urine samples at −70°C until analysis. The position of the catheter in the outer medulla was confirmed after sectioning of the right kidney.

Immunohistochemical Analysis of CB1. Kidneys were removed from a separate set of three wild-type mice, cut longitudinally, and fixed in 10% neutral buffered formalin. The fixed tissue was embedded in paraffin and sections were prepared. Immunostaining was performed as described previously (Ritter et al., 2012)using a rabbit polyclonal anti-CB1 antibodies directed at the first 99 amino acid residues of human CB1 (1:50, PA1-743; ThermoFisher Scientific). For comparison, sections were also stained using an antibody directed at the CB1 C-terminal residues 461–472 (1:50, ab23703; Abcam). Detection of goat anti-rabbit horseradish peroxidase–conjugated secondary antibody (111-035-003; Jackson Immunoresearch Laboratories) used diaminobenzidine as substrate (DAB Peroxidase Substrate Kit; Vector Laboratories, Burlingame, CA). For positive controls, sections were incubated with primary antibodies directed against NKCC2 (18970-1-AP; Proteintech) or aquaporin-2 (sc-9882; Santa Cruz). A negative control section was incubated only with secondary horseradish peroxidase–conjugated goat anti-rabbit antibody.

Western Blot Analysis. Western blot analysis was performed as described previously (Ritter et al., 2012). In brief, kidney cortical, outer medullary, and inner medullary tissue homogenates (15 μg/lane) from a separate group of two wild-type (WT) mice were

denatured and electrophoresed through a SDS-polyacrylamide gel electrophoresis followed by electro-blotting onto a polyvinylidene fluoride membrane. The membrane was probed sequentially with the anti-CB1 antibodies (1:500) or with anti-NKCC2 antibody (18970-1-AP, 1:500; Proteintech). After washing, the membranes were incubated for 1 hour with 1:3000 horseradish peroxidase-labeled secondary antibody. Images were developed using Amersham ECL Western Blot Detection reagent and recorded using a LI-COR Imaging System. To normalize for differences in protein loading, the blots were re-probed with a mouse monoclonal anti-β-actin primary antibody (1: 2000 dilution; Sigma-Aldrich).

Isolation of Mouse Renal mTALs. TAL tubules from WT and FAAH knockout (KO) mouse kidneys were isolated as described (Carroll et al., 2003) with the following modifications. Mice were anesthetized with thiobutabarbital and ketamine, and kidneys were perfused by intracardiac perfusion with HEPES–Hanks' balanced salt solution (HBSS; 138 mM NaCl, 5 mM KCl, 0.34 mM Na_2HPO_4, 0.44 mM KH_2PO_4, 1.3 mM $CaCl_2$, 0.5 mM $MgCl_2$, 4.2 mM $NaHCO_3$, 5.55 mM D-glucose, and 0.25 mM phenol red, and 10 mM HEPES, pH 7.4). Kidneys were removed and sectioned into coronal slices over ice. The inner stripe of the outer medulla was dissected and placed in HEPES-HBSS containing 0.1% collagenase. The tissue was sequentially digested in fresh changes of the above digestion solution for 10-minute periods at 37°C with oxygenation. At the end of each period, tissue was pipetted up and down and released tubules recovered by sedimentation of tissue for 30 seconds on ice. The supernatants were transferred into ice-cold HEPES-HBSS containing 1% bovine serum albumin. After filtration of the final tubule suspension through 53-μm nylon mesh (Fisher Scientific), tubules were recovered from the membrane, sedimented at 4C by centrifugation at 500*g*, and resuspended in ice-cold HEPES-HBSS.

$[Na^+]_i$ Measurement in mTAL Cells. Relative changes in $[Na^+]_i$ were monitored in mTAL cells by loading tubules isolated from mice with Na^+-sensitive fluoroprobe SBFI-AM (Cayman Chemical). The mTAL tubules were loaded with SBFI (10 μM) in the presence of 0.15% pluronic F-127 (a non-ionic copolymer surfactant; ThermoFisher Scientific) at 37°C for 2 hours. The mTAL cells were visualized through a Carl Zeiss MicroImaging, Inc. 40× (0.8 numerical aperture) or 60× (0.95 numerical aperture) objective with a Carl Zeiss MicroImaging, Inc. Axioskop 2 plus upright fluorescence microscope and imaged with a setup consisting of a charge coupled device camera (Imago, TILL Photonics; Applied Scientific Instrumentation, Eugene, OR) attached to an image intensifier (VS4-1845 Videoscope; Washington, DC), an epifluorescent light source (TILL Photonics Polychrome IV), a 515 nm dichroic beam splitter, and a 535 nm emission filter (20 nm band pass; Omega Optical). SBFI-loaded mTAL cells were alternately excited at 340 nm and 380 nm and imaged at 15-second intervals. Small regions of interest (ROIs) in the mTAL tubule (diameter 2 to 3 μm) were chosen in which the changes in the fluorescence intensity ratio (FIR; F_{340}/F_{380}) were analyzed using imaging software (TILLvisIon version 4.0.7.2; TILL Photonics). The background and autofluorescence at 340 nm and 380 nm were corrected from images of mTAL cells without the dye. All experiments were done at room temperature (~23°C).

The temporal changes in $[Na^+]_i$ were monitored in mTAL cells in response to a change in bath Na^+ concentration from 0 [0 Na^+ Ringer's solution (0 NaR)] to 140 mM Na^+ [control Ringer's solution (CR)]. The CR solution contained (in millimolars) 140 NaCl, 5 KCl, 1 $CaCl_2$, 1 $MgCl_2$, 10 glucose, 10 HEPES, pH 7.4. In 0 NaR solution, 140 mM NaCl was replaced with 140 mM *N*-methyl-D-glucamine, and the pH of the solution was adjusted to 7.4 with 1 N HCl. Temporal changes in $[Na^+]_i$ were also monitored in mTAL cells after the addition of CP, PF, AEA, URB, Ou, Bu, amiloride, or benzamil to the 0 NaR solutions or to the CR solutions. In some experiments, temporal changes in $[Na^+]_i$ were also monitored after a switch from 0 NaR solutions to CR solutions containing CP, PF, AEA, URB597, Ou, Bu, amiloride, or benzamil. Some of the drugs were first dissolved in DMSO or ethanol. Equivalent amounts of DMSO or ethanol were added to control solution.

Data Analysis. The relative changes in FIR were measured in each individual ROI within the tubule every 15 seconds. The FIR under control conditions for each ROI was taken as 1. The data were expressed as means ± S.E.M. of n, where n represents the number of ROIs within the mTAL tubule. The changes in FIR were compared between each ROI under different conditions. In some cases, the initial changes in FIR in each ROI were subjected to linear regression analyses to calculate the slope (ΔFIR/min). The data were also presented as means ± S.E.M. from different mTAL preparations. Student's t test was employed to analyze the difference between sets of data. Data were considered statistically significant when $P \leq 0.05$.

In vivo experimental data are also presented as the means ± S.E.M. of n, where n represents the number of animals used in the experiment. A one-way ANOVA was performed using a Dunnett's multiple comparison post hoc test when significant differences between treatment groups were found, using the first preinfusion control group, C1, or postrimonabant treatment P2 group as controls, as indicated. Data were considered statistically significant when $P \leq 0.05$.

Results

Stimulating Effect of Medullary AEA Infusion on Diuresis and Natriuresis in Mouse Kidney Is CB1-Dependent. We have previously demonstrated that AEA infused acutely into the right renal outer medulla of anesthetized mice induces diuresis and natriuresis from the infused kidney (Ritter et al., 2012). The effects of continuous intramedullary infusion of vehicle only (sham control) or vehicle containing AEA at increasing concentrations (15, 30, or 60 nmol/min per kilogram) on mean arterial pressure (MAP), urine flow rate, and urinary Na^+ excretion rate (UNa) in wild-type C57BL/6 mice are shown in Fig. 1A. As found previously, neither group showed any acute change in MAP from AEA, whereas urine flow rate was significantly elevated 92% and 108% by AEA at the 30 and 60 nmol/min per kilogram doses, respectively, versus the C1 control group. These elevations of urine flow were accompanied by significant increases in Na^+ excretion of 31% and 80% at the 30 and 60 nmol/min per kilogram AEA doses, respectively. To test the effect of rimonabant on the AEA-induced urine flow rate and UNa, a second group of mice received a rimonabant pretreatment (3 mg/kg i.p. bolus) 30 minutes prior to the start of the AEA infusions. These data are shown in Fig. 1B. The rimonabant pretreatment had the effects of decreasing MAP from 107 to 99 mm Hg ($P < 0.05$, C2 vs. P2 post-treatment period after rimonabant, respectively) and increasing UNa but not urine flow rate. The effect of rimonabant on MAP was prolonged. Subsequent addition of AEA to the intramedullary infusion solution had no significant effect on MAP, decreased urine flow rate from 13 to 4 μl/min per gram kidney weight at the 60 nmol/min per kilogram dose, and had no apparent effect on Na^+ excretion. These data demonstrate blockade of the effects of intramedullary AEA on urine flow rate and UNa by the CB1-selective inverse agonist, rimonabant.

Immunohistochemical and Western Blot Analyses of CB1 Receptor in Mouse Kidney. The distribution and tissue localization of CB1 receptor in mouse renal medulla was investigated by immunohistochemistry. Figure 2, A–C, presents images obtained using a CB1 amino-terminal–directed antibody (first 99 amino acids). Panel A represents a lower magnification (100×) of an image showing the junction between the inner and outer medulla. Tubules from the outer medulla showed

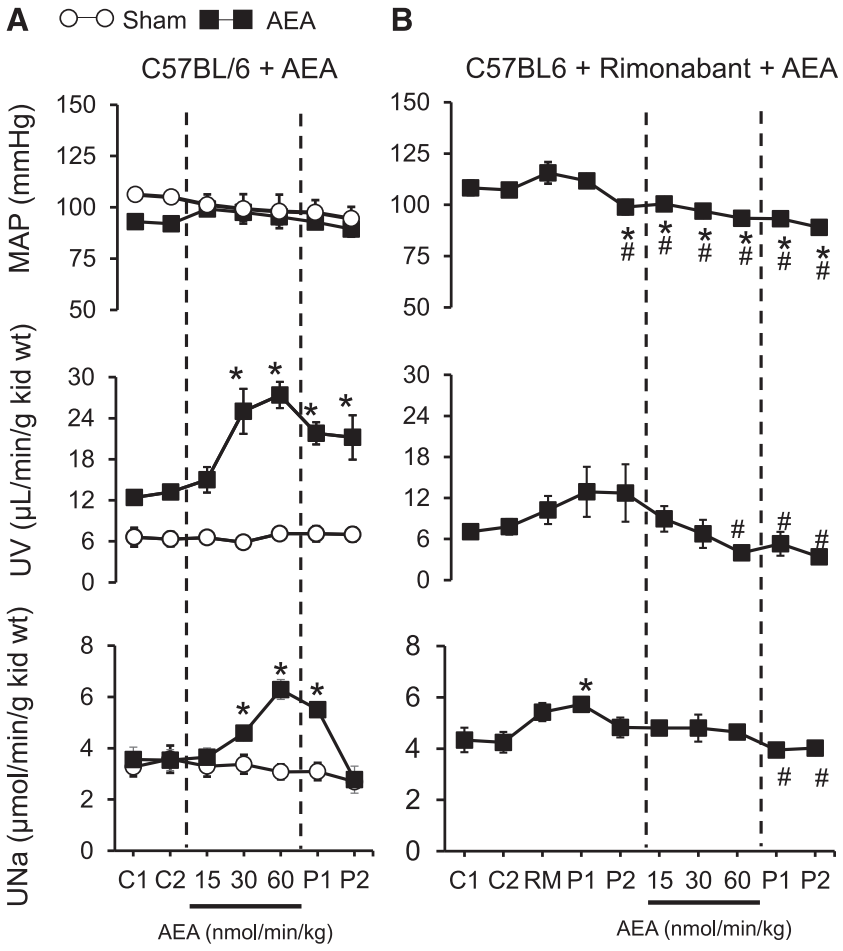

Fig. 1. The effect of intramedullary infusion of AEA on MAP, urine formation (UV), and UNa in wild-type mice with and without rimonabant (RM) pretreatment. The effects of AEA infusion at the indicated dose rates (in nanomoles per minute per milligram) on mean arterial pressure (top panels) or urine flow (bottom panels) are shown. C1 and C2 indicate the vehicle infusion control periods immediately prior to administration of AEA. P1 and P2 indicates the post-treatment control infusion periods. The animals in (A) received only AEA, whereas the animals in (B) received a pretreatment with RM (3 mg/kg i.p., 30 minutes prior to AEA). The data shown represent the means ± the S.E.M. of each period. $^{*}P < 0.05$ vs. the respective C1 control group; n = 5–7 per group. $^{\#}P < 0.05$ vs. the postrimonabant P2 group.

differential staining with the CB1 antibody compared with the inner medulla and to vasa recta bundles in the outer medulla. Higher power images of CB1 antibody-stained sections (Fig. 2, B and C) in the regions adjacent to vasa recta bundles are consistent with staining of thick ascending limb tubules and illustrate the primary intracellular and granular nature of CB1 staining. These results contrast with the differential apical distribution observed for NKCC2 (Fig. 2D) and aquaporin-2 (Fig. 2E). Essentially identical results were obtained using a carboxyl-terminal–directed CB1 antibody (data not shown). A negative control section labeled only with the secondary antibody did not show any positive staining (Fig. 2F).

Figure 3 presents Western blot analyses of total cortex, outer medulla, and inner medulla of wild-type mouse probed using antibodies directed at the CB1 amino (Fig. 3A) or carboxyl-terminal regions (Fig. 3B). The major band observed was identical in each case, migrating with an apparent size of 52 kDa. Both showed near equal staining in cortex and outer medulla with little CB1 detectable in inner medullary samples, consistent with the immunohistochemical data. In contrast, Western analysis using an NKCC2 antibody revealed two bands (180 and 150 kDa) with high selectivity for the outer medulla relative to the cortex or inner medulla (~180 kDa).

Effect of Bu on Na^+ Influx in mTAL Tubule Cells from WT Mice. The mTAL cells were first characterized by demonstrating the presence of Bu-sensitive Na^+ influx via NKCC2. In a representative experiment, in an mTAL tubule isolated from a WT mouse and loaded with SBFI (Fig. 4A; inset), replacing 0 NaR solution with CR solution induced a temporal increase in FIR in all 21 ROIs investigated. The mean FIR increased at the rate of 0.047 ± 0.002/min (Fig. 4; red regression line), and the maximum mean FIR increased from 1 to 1.21 ± 0.008 in ~12 minutes. When the Na^+-influx reached a plateau, CR was replaced with CR containing increasing concentrations of Bu (25, 50, and 100 µM) in a stepwise manner. Bu produced a rapid dose-dependent inhibition of the steady-state Na^+-influx in all mTAL tubule cells to near baseline (Fig. 4B). In seven individual mTALs (143 ROIs) isolated from seven mice, replacing 0 NaR with CR increased the mean FIR from 1 to 1.26 ± 0.03 (P = 0.0001; n = 7), and the FIR increased at the mean rate of 0.189 ± 0.039/min. These results indicate that adding Na^+ to the bathing solution induced a Na^+ influx into mTAL tubule cells.

In a separate mTAL isolated from a WT mouse, switching from 0 NaR to CR increased FIR from 1 to 1.46 ± 0.012 with an initial increase in slope (ΔFIR/min) of 0.246 ± 0.0038 (Supplemental Fig. 1A). Subsequently, switching from 0 NaR to CR + 50 µM Bu increased FIR from 1 to 1.26 ± 0.009 with an initial increase in slope (ΔFIR/min) of 0.098 ± 0.0019 (P = 0.0001; n = 33). Thus, Bu inhibited both the maximum increase in FIR and ΔFIR/min by 44% and 61%, respectively (P = 0.0001; n = 33) (Supplemental Fig. 1B). These results demonstrate the presence of the Bu-sensitive Na^+ influx via NKCC2 in mTAL tubule cells. All tubules used in this study were characterized as mTALs by the presence of Bu-sensitive Na^+ flux (Figs. 5–11).

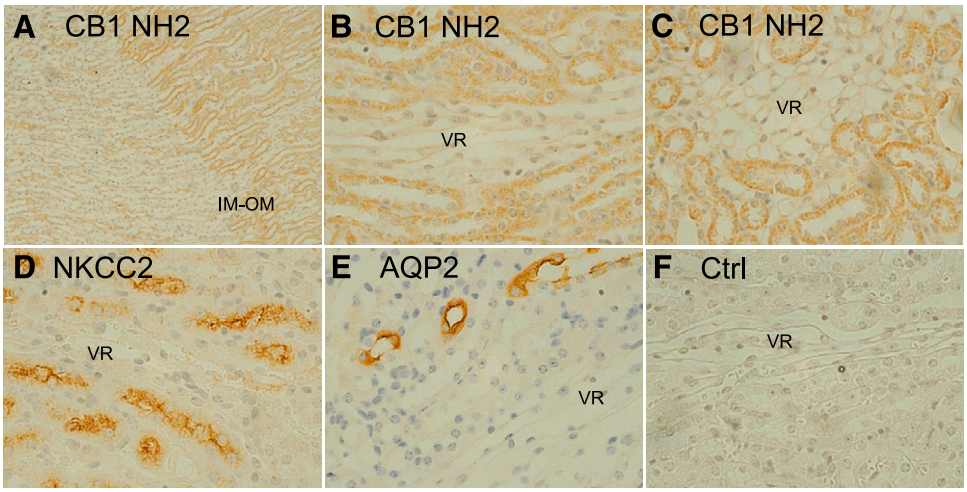

Fig. 2. Immunohistochemical localization of CB1 distribution in outer and inner medulla of mouse kidney. Sections of formalin-fixed, paraffin-embedded FAAH wild-type mouse kidneys were processed for immunohistochemical analysis as described under *Materials and Methods* using the primary antibodies indicated. CB1 NH_2 terminus (A–C), NKCC2 (D), aquaporin-2 (AQP2) (E), and no primary antibody control (Ctrl) (F). All images are 400× except A (original magnification, 100×). Images correspond to the inner stripe of the outer medulla (OM) except (A), which shows the junction between the inner medulla (IM) and outer medullas. Brown color represents positive staining for the horseradish peroxidase–conjugated secondary antibody detected using diaminobenzidine, whereas blue color represents staining for nuclei/nucleic acid by Mayer's hematoxylin. Tubules of the inner stripe of the outer medulla including thick ascending limb and collecting ducts showed differential CB1 staining relative to either inner medullary tubules or vasa recta (VR) bundles of the outer medulla. Staining with the CB1 COOH-terminal antibody produced similar results.

Effect of CP on Na^+ Influx in mTAL Tubules Isolated from WT Mice. The mTAL tubules were isolated, and the effect of the synthetic CBR agonist, CP, on Na^+ influx was investigated. CP mimics the effects of the naturally occurring THC (Little et al., 1988; Pertwee, 1999). In mTAL tubule cells loaded with SBFI (Fig. 5; inset), switching from 0 NaR to CR, the cells responded with a reversible increase in maximum FIR. FIR increased from 1 to 1.31 ± 0.01 with an initial increase in slope (ΔFIR/min) of 0.22 ± 0.006 (Fig. 5). Switching from 0 NaR to 0 NaR + 10 μM CP did not induce a significant change in FIR over a period of ~10 minutes. Upon switching to CR containing 10 μM CP, FIR in mTAL tubule cells increased rapidly from 1 to 1.47 ± 0.01 with an increase in initial slope (ΔFIR/min) of 0.19 ± 0.0048 (Fig. 5). The maximum increase in FIR in the presence of CR + CP was 51.6% greater than that induced by CR alone (P = 0.0001; n = 23). The increase in initial slope in the presence of CR + CP was only 13.5% less than that obtained in the presence CR alone (P = 0.003; n = 23). These results suggest that CP produces a time-dependent increase in $[Na^+]_i$ in mTAL cells by a mechanism that does not involve an initial increase in Na^+-influx via the Bu-sensitive NKCC2 (Fig. 4).

Similar to the results shown in Fig. 5, in the second part of Supplemental Fig. 1, following the removal of external Na^+ in the presence of CP decreased the FIR close to the baseline value. These results further demonstrate that CP effects are inhibited in the absence of external Na^+.

Effect of CP on Steady State $[Na^+]_i$ in mTAL Tubule Cells from WT Mice. We next tested if CP can increase steady state $[Na^+]_i$ in mTAL cells pre-equilibrated in CR. In an additional mTAL tubule, switching from CR to CR + 10 μM CP also induced a time-dependent increase in FIR (Fig. 6). In CR without CP, FIR was 1.17 ± 0.011, and in the presence of CR + CP, FIR increased to 1.55 ± 0.018 (P = 0.0001; mean ± S.E.M.; N = 27; mean ΔFIR = 0.38). Immediately after CP exposure, FIR increased at a rate of 0.0027 ± 0.0004/min, and after 19 minutes of CP exposure FIR increased at the rate of 0.0062 ± 0.0002/min (P = 0.0001). In four independent mTALs (90 ROIs) isolated from four mice, adding CP to CR induced maximum increase in FIR by 0.308 ± 0.051 (P = 0.02; n = 4). These results indicate that CP induces a time-dependent increase in $[Na^+]_i$ in mTAL tubule cells under normal physiologic conditions (i.e., in CR).

Effects of CP on $[Na^+]_i$ in mTAL Tubule Cells Are Independent of NKCC2. As shown in the last part of Fig. 4, when CR + 100 μM Bu solution was changed to CR + 100 μM Bu + 10 μM CP, CP produced a delayed time-dependent increase in $[Na^+]_i$ in mTAL tubule cells. Upon immediate addition of CP, FIR increased at the rate of 0.0033 ± 0.00038/min. However, after an 11-minute exposure after CP, FIR increased at the rate of 0.01 ± 0.0004/min (Fig. 4; red regression lines; P = 0.0001), and the maximum mean FIR increased from 1 to 1.32 ± 0.0055 in 45 minutes. This increase in FIR was significantly higher (P = 0.0001) than the maximum increase in FIR (1.21 ± 0.008) induced by replacing 0 NaR with CR. These results indicate that the effects of CP are delayed and occur at a slower time frame. The CP-induced mean maximum increase in FIR (0.32) in the presence of Bu is similar to the mean increase in FIR in four mTALs in the absence of Bu (0.308 ± 0.051). Most importantly, these results indicate that the CP-induced increase in Na^+ influx in mTAL cells is Bu-insensitive and does not involve Na^+ influx via the apical NKCC2.

CP Alters $[Na^+]_i$ in mTAL Tubule Cells by Blocking Na^+-K^+-ATPase. CP effects on $[Na^+]_i$ in mTAL tubule cells were not dependent upon an increase in initial Na^+-influx via NKCC (Fig. 4) and were not observed when Na^+ was removed from the external medium (Fig. 5). We hypothesize that in the absence of external Na^+, mTAL cells do not transport Na^+, and Na^+-K^+-ATPase is nonfunctional. Accordingly, we next tested if CP increases $[Na^+]_i$ in mTAL tubule cells by inhibiting Na^+-K^+-ATPase in the presence of external Na^+. Ou was used to block Na^+-K^+-ATPase activity in the basolateral membrane of mTAL tubule cells. As shown in Fig. 7, switching from CR to

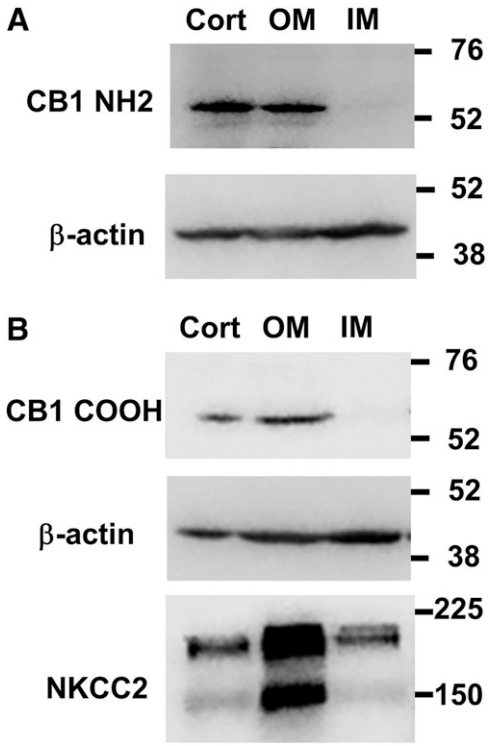

Fig. 3. Western blot analysis of CB1 receptor distribution in mouse kidney. Tissue from renal cortex, outer medulla, and inner medulla from mouse kidney was dissected, homogenized in Tris-buffered EDTA and glycerol, and analyzed for protein content. Total protein (15 μg) was electrophoresed using SDS-PAGE gels in parallel with molecular size markers (Amersham Rainbow full range). After electrotransfer, blots were probed for either NKCC2 or the amino or carboxyl termini of CB1 at 1: 1000 dilutions as described under *Materials and Methods*. After ECL detection, blots were reprobed using a mouse anti-*β*-Actin monoclonal antibody to normalize for differences in protein loading.

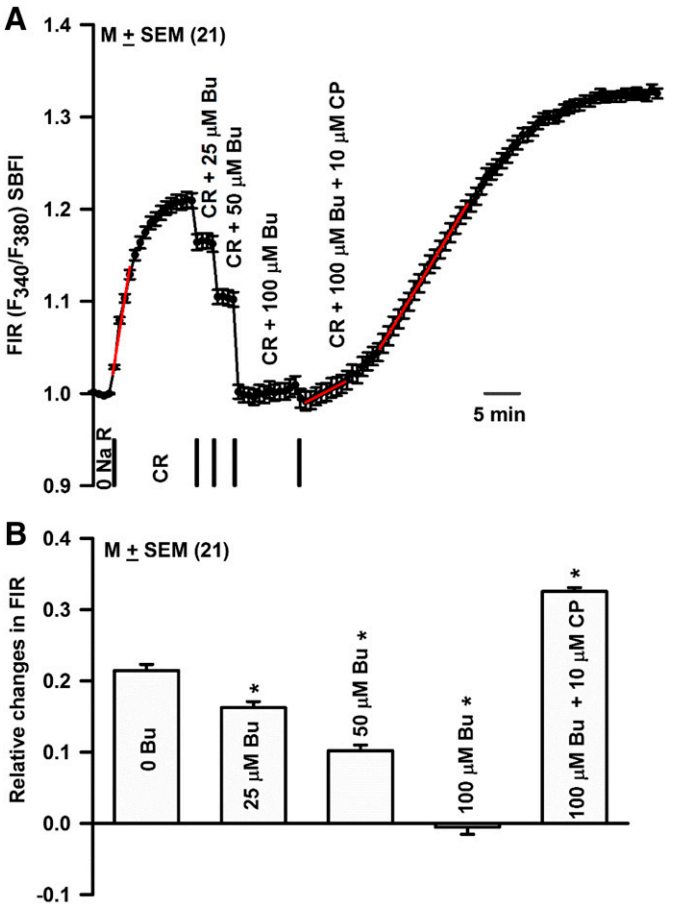

Fig. 4. Effect of Bu and CP on Na^+ influx in an mTAL isolated from a WT mouse. (A) An mTAL tubule was loaded with SBFI and was initially perfused with 0 NaR (pH 7.4) containing 140 mM *N*-methyl-D-glucamine–Cl. In the first step, 0 NaR was replaced with the CR solution (pH 7.4) containing 140 mM NaCl. Changes in Na^+ flux were measured as temporal changes in FIR (F_{340}/F_{380}). When FIR reached a plateau, CR was sequentially replaced with CR containing increasing concentrations of Bu (25, 50, and 100 μM). In the final step, CR + 100 μM Bu solution was replaced with CR + 100 μM Bu + 10 μM CP solution for the remainder of the experiment. The mean ± S.E.M. FIR values were calculated from 21 ROIs. Vertical bars represent the time periods when different solutions were switched during the experiment. The red lines in the figure represent linear regression lines and the initial increase in slope in response (Δ FIR/min) to a change from 0 NaR to CR and then from CR + Bu to CR + Bu + CP. (B) The relative changes in FIR from baseline (0 NaR) under different Bu concentrations and in the presence of Bu + CP. *P = 0.0001 (n = 21).

CR + 2 mM Ou induced a time-dependent increase in FIR. After Ou exposure, FIR increased from 1.22 ± 0.012 to its maximum value 1.37 ± 0.017 (P = 0.0001; N = 18; mean ΔFIR = 0.15) in 13 minutes. Immediately after Ou exposure, FIR increased at the rate of 0.016 ± 0.0005/min (Fig. 7; red line). In three individual mTALs (54 ROIs) from three mice, adding Ou to the CR increased ΔFIR by 0.213 ± 0.036 (P = 0.0042; n = 3). These results indicate that in mTAL tubule cells, inhibition of Na^+-K^+-ATPase activity results in a time-dependent increase in $[Na^+]_i$.

In an mTAL isolated from a WT mouse, adding Ou to the CR also produced a slow time-dependent increase in FIR (Supplemental Fig. 2) from 1.013 ± 0.002 to 1.156 ± 0.007 (ΔFIR = 0.143; P = 0.0001; n = 18). Adding Bu (100 μM) to the CR + Ou solution inhibited the Na^+ influx below baseline (0.806 ± 0.00142; P = 0.0001) almost instantaneously. These results indicate that similar to the case with CP (Figs. 5 and 6), Ou-induced increase in Na^+ in mTAL cells does not significantly affect Na^+ influx via the apical NKCC.

In Fig. 5, after CP treatment, adding Ou to the bathing solution increased FIR from 1.46 ± 0.01 to 1.50 ± 0.01 in 12 minutes with an initial value of ΔFIR/min of 0.0047 ± 0.00033 (N = 23). In Fig. 6, after CP treatment, adding Ou to the bathing solution increased FIR from 1.52 ± 0.02 to 1.60 ± 0.01 in 10 minutes with an initial value of ΔFIR/min of 0.0082 ± 0.00054 (N = 27). In Fig. 7, after Ou treatment, adding CP to the bathing solution increased FIR from 1.37 ± 0.02 to 1.46 ± 0.02 (ΔFIR = 0.09) in 36 minutes with an initial ΔFIR/min value of 0.0041 ± 0.00026 (N = 18). Figure 8A shows that summary of the results of the effects of CP, Ou, and CP + Ou obtained in Figs. 5–7 and 10 (see below) as bar graphs. The data were combined and analyzed in Fig. 8B. The results show that adding CP or Ou to CR produced a mean increase in FIR by 0.228 ± 0.063 (n = 4). In contrast, adding Ou after CP or adding CP after Ou only produced a mean increase in FIR by 0.043 ± 0.015 (*P = 0.0001; n = 3). Taken together, the above results suggest that Ou attenuates the effect of CP and, in turn, CP attenuates the effects of Ou on $[Na^+]_i$ in mTAL tubule cells by inhibiting Na^+-K^+-ATPase.

Effect of PF3845 on $[Na^+]_i$ in mTAL Tubule Cells Isolated from WT Mice. Results shown in Figs. 4–8 demonstrate that CP, a synthetic nonselective CBR agonist, modulates changes in $[Na^+]_i$ in mTAL tubule cells by inhibiting

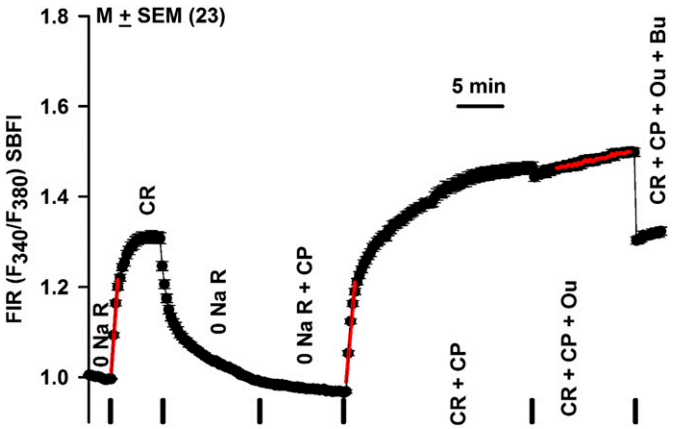

Fig. 5. Effect of CP, Ou, and Bu on Na^+ influx in mTALs isolated from WT mouse. An mTAL tubule isolated from WT mouse and loaded with SBFI was initially perfused with 0 NaR. In the first step, 0 NaR was replaced with CR. In the second step, CR was again replaced with the 0 NaR. In the third step, 0 NaR was replaced with 0 NaR + 10 μM CP. In the fourth step, 0 NaR + 10 μM CP was replaced with CR + 10 μM CP. To test if changes in FIR were sensitive to Ou or Bu, CR + 10 μM CP solution was replaced with CR + 10 μM CP + 10 mM Ou and then with CR + 10 μM CP + 10 mM Ou + 50 μM Bu. Changes in Na^+ flux was measured as temporal changes in FIR (F_{340}/F_{380}). The mean ± S.E.M. FIR values are calculated from 23 ROIs. Vertical bars represent the time periods when different solutions were switched during the experiment. The red lines in the figure represent linear regression lines and the initial increase in slope (Δ FIR/min) in response to change from 0 NaR to CR and then from 0 NaR + CP to CR + CP.

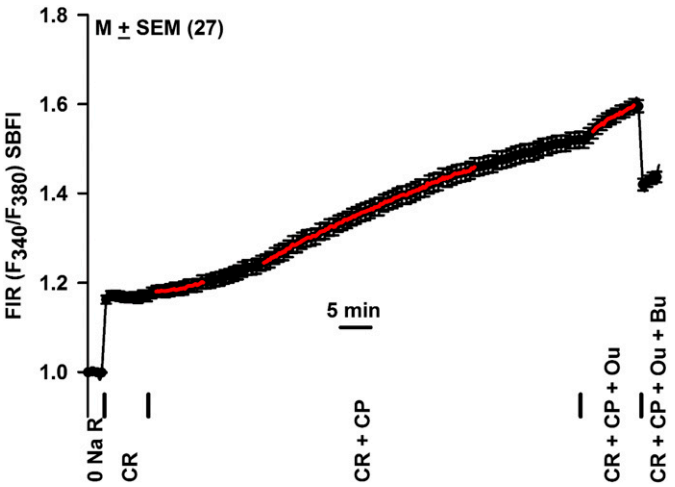

Fig. 6. Effect of CP, Ou, and Bu on resting $[Na^+]_i$ in mTALs isolated from WT mice. An mTAL tubule isolated from a WT mouse and loaded with SBFI was initially perfused with 0 NaR. In the next step, 0 NaR was replaced with CR and then with CR + 10 μM CP. To test if changes in $[Na^+]_i$ were sensitive to Ou or Bu, CR + 10 μM CP solution was replaced with CR + 10 μM CP + 10 mM Ou and then with CR + 10 μM CP + 10 mM Ou + 50 μM Bu. Changes in $[Na^+]_i$ were measured as temporal changes in FIR (F_{340}/F_{380}). The mean ± S.E.M. FIR values are calculated from 27 ROIs. Vertical bars represent the time periods when different solutions were switched during the experiment. The red lines in the figure represent linear regression lines and the increase in slope (Δ FIR/min) after immediate and 19-minute exposure to CR + CP.

basolateral Na^+-K^+-ATPase activity. In the next set of experiments, we tested if endogenous endocannabinoid can also modulate $[Na^+]_i$ in mTAL tubule cells. PF is a potent, irreversible inhibitor of FAAH, the principal enzyme involved in the degradation of the endocannabinoid, AEA, to arachidonic acid + ethanolamine. Inhibition of FAAH by PF is expected to increase AEA in mTAL tubule cells. Accordingly, we next treated mTAL tubule cells with PF. In an isolated mTAL tubule from a WT mouse (Fig. 9), switching from CR to CR + 10 μM PF, after about 5 minutes' delay, PF induced a time-dependent increase in FIR from 1.25 ± 0.02 to 1.52 ± 0.03 ($P = 0.0001$; $N = 11$; mean ΔFIR = 0.27) in 52 minutes. After a 5-minute delay, the initial ΔFIR/min increased by 0.01 ± 0.00055. In the next step, switching from CR + 10 μM PF to CR + 10 μM PF + 10 mM Ou did not increase FIR above 1.52 ± 0.03 ($N = 11$) in 6 minutes (Fig. 9). Taken together, the above results suggest that both exogenous (CP) and endogenous (AEA) cannabinoids produce temporal increase in $[Na^+]_i$ in mTAL tubule cells by inhibiting Na^+-K^+-ATPase.

Effects of CP on $[Na^+]_i$ in mTAL Tubule Cells Are Independent of FAAH. To test if the effects of CP on $[Na^+]_i$ in mTAL tubule cells are independent of FAAH, additional experiments were performed in mTAL tubules isolated from a FAAH KO mouse. In these experiments, instead of using PF, we used URB, a relatively selective inhibitor of FAAH. As shown in Fig. 10, switching from CR to CR + 1 μM URB produced only a small change in FIR from 1.23 ± 0.02 to 1.28 ± 0.02 ($n = 11$; mean ΔFIR = 0.05) in 20 minutes. These changes are very small and statistically insignificant. These results confirm the absence of FAAH in KO mice. Similar to the results shown in Figs. 4 and 6, switching to CR + URB + CP, after a delay of 2 minutes, CP induced a time-dependent increase in FIR from 1.28 ± 0.02 to 1.65 ± 0.01 ($P = 0.0001$; $N = 11$; mean ΔFIR = 0.37) in 22 minutes. The effects of CP in FAAH KO mice are comparable to the effects of CP shown in Figs. 4 and 6. CP induced an initial increase in ΔFIR/min of 0.0341 ± 0.0014. Also, similar to the data shown in Figs. 5–7, after CP treatment, exposure to Ou for 5 minutes did not further increase FIR above 1.65 (Fig. 10). These results indicate that CP effects on $[Na^+]_i$ in mTAL tubule cells are independent of FAAH activity.

Effects of AEA on $[Na^+]_i$ in mTAL Tubule Cells Are Independent of FAAH. As shown in Fig. 11, in an mTAL tubule isolated from a FAAH KO mouse, 10 μM PF produced only a small but transient change in FIR (1.38 ± 0.02 to 1.42 ± 0.02; ΔFIR = 0.04; $N = 24$). Relative to the effect of PF in WT mice (Fig. 9), both PF and URB (Fig. 10) produce very small changes in FIR over a period of 10–15 minutes, further confirming that KO mice do not have residual FAAH activity. Subsequently treating mTAL tubule cells with 20 μM AEA induced a time-dependent increase in FIR from 1.42 ± 0.02 to 1.65 ± 0.01 (ΔFIR = 0.23; $P = 0.0001$; $N = 24$). AEA induced an initial increase in ΔFIR/min of 0.0084 ± 0.00048. These results indicate that in WT mice (Fig. 9), PF inhibits FAAH and produces its effects by increasing AEA in mTAL tubule cells. After AEA treatment, a 5-minute exposure to Ou did not further increase FIR. This indicates AEA also produces a temporal increase in $[Na^+]_i$ in mTAL tubule cells by inhibiting Na^+-K^+-ATPase.

Effects of CP on $[Na^+]_i$ in mTAL Tubule Cells Are Blocked by Rimonabant. We tested if rimonabant (RIM) can also block the effects of CP on intracellular sodium in the in vitro tubule model. As shown in Fig. 12, in an mTAL tubule isolated from a FAAH KO mouse, changing from 0 NaR to CR produced the usual rapid increase in FIR. Adding 10 μM RIM to CR increased the mean FIR from 1.10 ± 0.056 in CR to 1.12 ± 0.009 in ~20 minutes. These results indicate that by itself RIM does alter resting $[Na^+]_i$ in mTAL cells. In the continuous presence of RIM, CP (10 μM) also only increased FIR to 1.14 ± 0.009 in ~20 minutes. These results indicate that RIM inhibits the

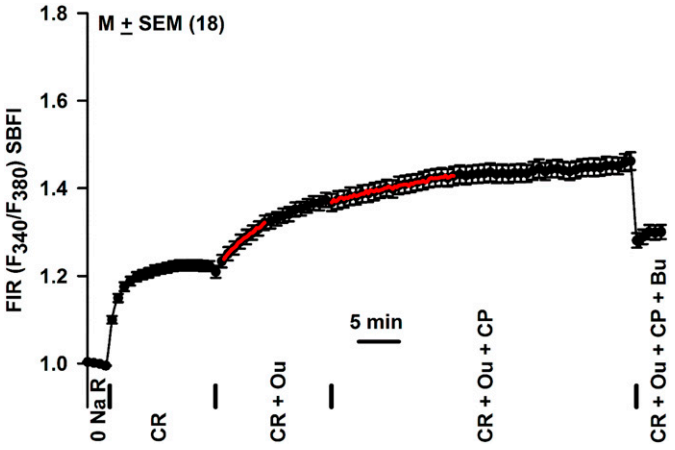

Fig. 7. Effect of Ou and Ou + CP on resting $[Na^+]_i$ in mTALs isolated from WT mouse. An mTAL tubule isolated from WT mouse and loaded with SBFI was initially perfused with 0 NaR. In the first step, 0 NaR was replaced with CR. In the second step, CR was replaced with CR + 10 mM Ou. In the third step, CR + 10 mM Ou was replaced with CR + 10 mM Ou + 10 μM CP and then with CR + 10 mM Ou + 10 μM CP + 50 μM Bu. Changes in $[Na^+]_i$ were measured as temporal changes in FIR (F_{340}/F_{380}). The mean ± S.E.M. FIR values are calculated from 18 ROIs. Vertical bars represent the time periods when different solutions were switched during the experiment. The red line in the figure represent linear regression lines and the increase in slope (Δ FIR/min) after exposure to CR + Ou.

CP-induced increase in FIR observed in Figs. 4–6 and 10. In the next step, adding Ou to the CR + RIM + CP solution produced a time-dependent increase in FIR from 1.14 ± 0.009 to 1.31 ± 0.02 (P = 0.0001). This Ou-induced mean increase in FIR (0.17) is similar to the effect of Ou (0.15) shown in Fig. 7. These results indicate that blocking CB receptors by RIM blocks the effects of CP on Na^+-K^+-ATPase.

Discussion

Cannabinoids have been demonstrated to stimulate urine flow accompanied by increased Na^+ excretion in laboratory animal models (Sofia et al., 1977; Ritter et al., 2012; Chopda et al., 2013; Paronis et al., 2013), but the mechanism has remained unclear. Silva et al. reported that AEA inhibited oxygen consumption in rat TAL tubules, consistent with an inhibitory effect on Na^+ transport (Silva et al., 2013). They showed this effect also occurred with WIN55212-2, a synthetic CBR agonist, and was blocked by rimonabant, a CB1 inverse agonist. The finding that AEA had no effect on oxygen consumption in TALs treated with Na^+ entry inhibitors led the investigators to conclude that the effect of AEA was on Na^+ transport rather than inhibition of oxidative phosphorylation. In this study, we used an alternative approach to study Na^+ transport in TALs, the use of the Na^+-sensitive dye, SBFI-AM, to monitor changes in $[Na^+]_i$ (Yu et al., 2007). The data obtained in our study are consistent with the inhibition of Na^+-K^+-ATPase by cannabinoids in the mechanism of altered Na^+ transport.

Previously we reported that infusion of either AEA, a direct-acting cannabinoidimetic, or PF, an indirect-acting cannabinoidimetic that elevates AEA indirectly by inhibiting FAAH, into the renal outer medulla of mice acutely stimulates diuresis and natriuresis (Ritter et al., 2012; Ahmad et al., 2018). This study addressed the role of CB1 by testing the effect of rimonabant on these effects in vivo. Our finding that rimonabant blocks the AEA effects (Fig. 1) is consistent with CB1 mediating diuresis and natriuresis (Chopda et al., 2013; Silva et al., 2013). The dose of rimonabant (3 mg/kg i.p.) selected for our study has been used by others to provide evidence of CB1-selective effects (Wise et al., 2007).

Our immunohistochemical localization data are the first, to our knowledge, to address the distribution of the CB1 receptor in the renal medulla (Park et al., 2017). Immunohistochemical staining with a CB1 antibody revealed a clear line of demarcation at the junction of the inner and outer medullas (Fig. 2A), suggestive of lower CB1 levels in the inner medulla. The latter finding is supported by the Western blot data (Fig. 3, A and B). Although our results demonstrate the presence of CB1 localization in TAL tubules, the differences

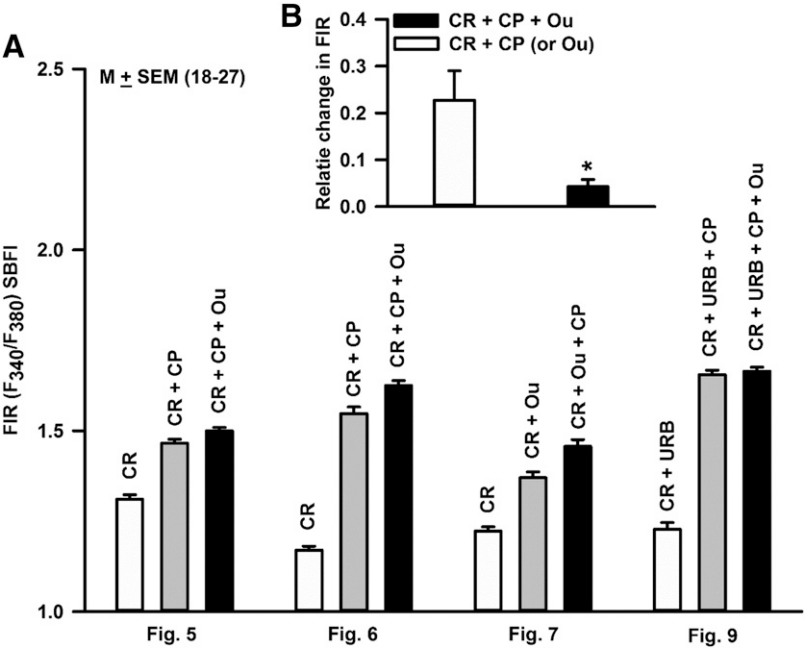

Fig. 8. Summary of the data on the effects of Ou, CP, and CP + Ou. (A) Changes in maximum FIR values in Figs. 5–7 and 9 are plotted as bar graphs. (B) Mean maximum changes in FIR in the presence of CR + CP (or Ou) were combined and compared with FIR values in the presence of CR + CP + Ou. *P = 0.0001 (unpaired; n = 4).

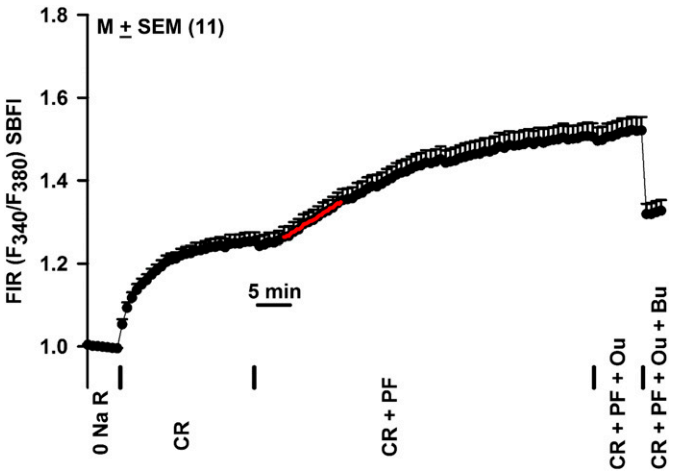

Fig. 9. Effect of the FAAH inhibitor, PF, and PF + Ou on resting $[Na^+]_i$ in mTALs isolated from WT mouse. An mTAL tubule isolated from WT mouse and loaded with SBFI was initially perfused with 0 NaR. In the first step, 0 NaR was replaced with CR. In the second step, CR was replaced with CR + 10 μM PF. In the third step, CR + 10 μM PF was replaced with CR + 10 μM PF + 10 mM Ou and then with CR + 10 μM PF + 10 mM Ou + 50 μM Bu. Changes in $[Na^+]_i$ were measured as temporal changes in FIR (F_{340}/F_{380}). The mean ± S.E.M. FIR values are calculated from 11 ROIs. Vertical bars represent the time periods when different solutions were switched during the experiment. The red lines in the figure represent linear regression line and the initial increase in slope (Δ FIR/min) after exposure to CR + PF.

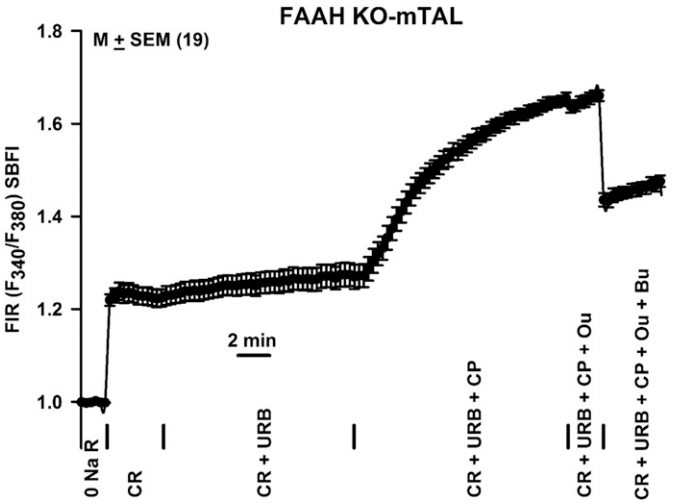

Fig. 10. Effect of the FAAH inhibitor, URB, and URB + CP55940 on resting $[Na^+]_i$ in mTALs isolated from FAAH KO mouse. An mTAL tubule isolated from FAAH KO mouse and loaded with SBFI was initially perfused with 0 NaR. In the first step, 0 NaR was replaced with CR. In the second step, CR was replaced with CR + 1 μM URB, and then with CR + 1 μM URB + 10 μM CP. In the final step, CR + 1 μM URB + 10 μM CP solution was replaced with CR + 1 μM URB + 10 μM CP + 10 mM Ou and then with CR + 1 μM URB + 10 μM CP + 10 mM Ou + 50 μM Bu. Changes in $[Na^+]_i$ were measured as temporal changes in FIR (F_{340}/F_{380}). The mean ± S.E.M. FIR values are calculated from 19 ROIs. Vertical bars represent the time periods when different solutions were switched during the experiment. The red lines in the figure represent linear regression line and the initial increase in slope (Δ FIR/min) after exposure to CR + URB + CP.

observed using specific marker antibodies, NKCC2 and aquaporin-2, for TALs and collecting ducts suggest that other nephron segments are also CB1-positive. This result implies that other tubular segments in the cortex and outer medulla besides the thick ascending limb may contribute to the mechanism of cannabinoid-induced diuresis. The observation that CB1 staining in outer medullary tubular cells is primarily intracellular and granular in nature suggests an intracellular mechanism of CB1-induced diuresis. CB1 has been reported in multiple intracellular organelles, including endosomes (Hsieh et al., 1999; Leterrier et al., 2004), lysosomes (Brailoiu et al., 2011; Rozenfeld, 2011), and mitochondria (Bénard et al., 2012). These results are consistent with CB1 mediating the effects of cannabinoids in the renal medullary TAL tubules.

Our study extended the findings of Silva et al. (2013) by using a complementary approach to study the effects of cannabinoids on sodium transport in TAL cells, employing the fluorescent Na^+-sensitive dye approach to monitor changes in $[Na^+]_i$. Our data reproducibly demonstrated that the addition of cannabinoid to the bathing solution caused $[Na^+]_i$ to increase in TAL cells (e.g., in Fig. 5, maximum FIR of 1.47 for CR + CP vs. 1.31 for CR alone, $P < 0.0001$). Compared with the elevation after the switch from 0 NaR to medium containing 140 mM (CR), this increase was delayed in onset and slow. In addition, it occurred in the presence of Bu, an NKCC2 inhibitor. These results collectively indicate that the mechanism of CBR-mediated inhibition of Na^+ transport in TAL cells does not involve inhibition of Na^+ entry mechanisms (Silva et al., 2013).

Alternatively, our data indicate that the elevation of $[Na^+]_i$ induced by cannabinoid treatment is due to inhibition of Na^+ exit via Na^+-K^+-ATPase. This interpretation is based on observations of the Bu-insensitivity of the effect and on evidence for functional interaction showing mutual complementary effects of Ou and cannabinoidimetics. When the effect of a maximum Na^+-K^+-ATPase-inhibiting concentration of Ou (2 mM) on $[Na^+]_i$ was allowed to approach plateau, the cannabinoidimetic-induced effects were significantly reduced (Figs. 7 and 8). Likewise, when the $[Na^+]_i$-elevating effect of CP, AEA, or PF were allowed to approach maximum, Ou was without further significant effects (Figs. 8 and 9). Like the cannabinoidimetics, Ou and other cardiotonic glycoside Na^+-K^+-ATPase inhibitors are recognized diuretic agents (Loreaux et al., 2008; Askari, 2019). The observed differences in the kinetics of $[Na^+]_i$ accumulation by Ou and cannabinoids suggest that different mechanisms are involved. Ou exerts its effect through direct binding to the Na^+-K^+-ATPase enzyme (Loreaux et al., 2008). Kinetically, the effect of Ou was monotonic with a rapid onset (Fig. 7). In contrast, CP showed evidence of a multiphasic effect with an initial slow rate of $[Na^+]_i$ accumulation followed by a delayed increase in rate (Figs. 4 and 6). This delayed onset of effect is consistent with an indirect mechanism initiated by binding to CBR, activation of G proteins, and signaling to downstream targets (Howlett and Abood, 2017). The present study did not address whether the effect of cannabinoids is associated with reduced Na^+-K^+-ATPase activity of TAL cell membrane fractions. Sampaio et al. have previously investigated the effects of cannabinoids on Na^+-K^+-ATPase activity of pig kidney proximal tubule LLC-PK1 cells. Treatment with the CBR agonist, WIN 55212-2, increased, whereas a CB1 inverse agonist (hemopressin) decreased Na^+-K^+-ATPase activity measured by the malachite green method (Sampaio et al., 2015), effects opposite to our observations. It may be that the cannabinoidimetic-induced inhibition of Na^+-K^+-ATPase is specific for TAL versus proximal tubule cells, represents a species difference, or, alternatively, indicates an indirect action mediated through diminished mitochondrial production of ATP levels or altered mitochondrial localization (Drori et al., 2019).

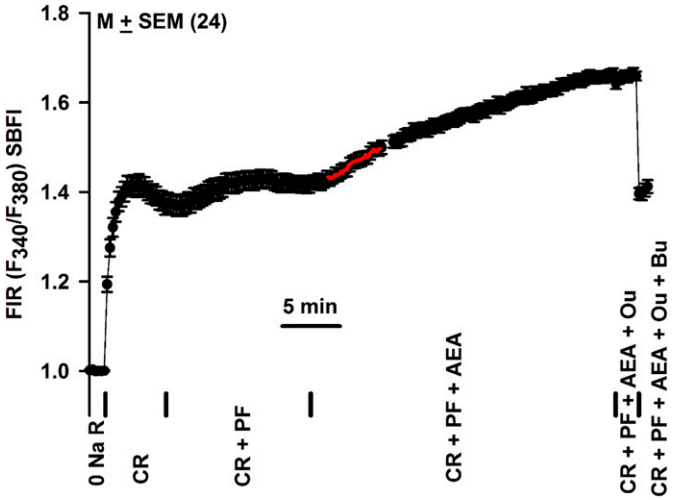

Fig. 11. Effect of PF and PF + AEA on resting $[Na^+]_i$ in mTALs isolated from FAAH KO mouse. An mTAL tubule isolated from FAAH KO mouse and loaded with SBFI was initially perfused with 0 NaR. In the first step, 0 NaR was replaced with CR. In the second step, CR was replaced with CR + 10 μM PF and then with CR + 10 μM PF + 20 μM AEA. In the final step, CR + 10 μM PF + 20 μM AEA solution was replaced with CR + 10 μM PF + 20 μM AEA + 10 mM Ou and CR + 10 μM PF + 20 μM AEA + 10 mM Ou + 50 μM Bu. Changes in $[Na^+]_i$ were measured as temporal changes in FIR (F_{340}/F_{380}). The mean ± S.E.M. FIR values are calculated from 24 ROIs. Vertical bars represent the time periods when different solutions were switched during the experiment. The red lines in the figure represent linear regression line and the initial increase in slope (Δ FIR/min) after exposure to CR + PF + AEA.

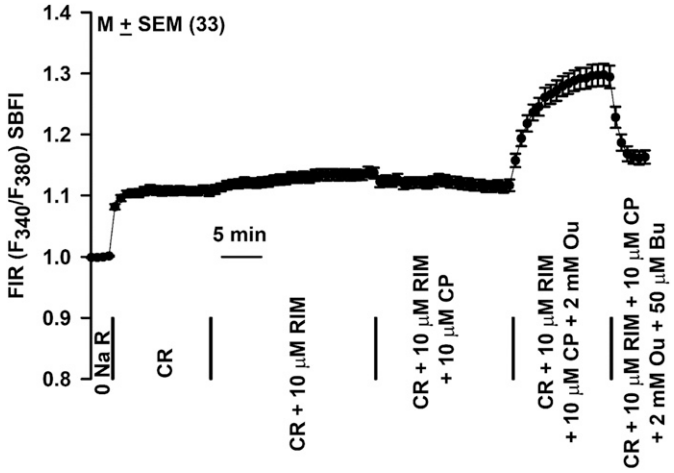

Fig. 12. Effect of RIM and RIM + CP on resting $[Na^+]_i$ in mTALs isolated from FAAH KO mouse. An mTAL tubule isolated from FAAH KO mouse and loaded with SBFI was initially perfused with 0 NaR. In the first step, 0 NaR was replaced with CR. In the second step, CR was replaced with CR + 10 μM RIM and then with CR + 10 μM RIM + 10 μM CP. In the final steps, CR + 10 μM RIM + 10 μM CP solution was replaced with CR + 10 μM RIM + 10 μM CP + 2 mM Ou and then CR + 10 μM RIM + 10 μM CP + 2 mM Ou + 50 μM Bu. Changes in $[Na^+]_i$ were measured as temporal changes in FIR (F_{340}/F_{380}). The mean ± S.E.M. FIR values are calculated from 24 ROIs. Vertical bars represent the time periods when different solutions were switched during the experiment.

This study also examined the effect of FAAH inhibitors on accumulation of intracellular Na^+ in TAL cells. Members of this pharmacologic class, which includes the investigational drug, PF, may be viewed as indirect cannabinoidimetics in that they indirectly promote cannabinoid signaling through accumulation of AEA. As observed for AEA, PF induced diuresis and natriuresis after its infusion into the renal medullas of mice (Ahmad et al., 2018). The results of this study show that, as predicted, PF treatment also resulted in elevation of intracellular Na^+, and that its effect is dependent on the presence of functional FAAH in the TAL tubules. It occurred in TALs from WT mice (Fig. 8) but to a reduced extent in tubules from FAAH KO mice (Fig. 11). Moreover, the addition of AEA to the FAAH KO tubules treated with PF overcame this lack of effect. Similar results were obtained using a second FAAH inhibitor, URB, in the absence and presence of CP55940 (Fig. 10). These data suggest that the $[Na^+]_i$-elevating effect of the FAAH inhibitor, PF, in the WT TALs is attributable to accumulation of the endogenous cannabinoid, AEA, signifying the presence of a basal endocannabinoid tone in cultured tubules. The existence of such a basal endocannabinoid tone was previously suggested by us to exist in the mouse renal medulla based on the observed in vivo stimulation of diuresis and natriuresis by intramedullary infused PF (Ahmad et al., 2018). The mechanism(s) responsible for stimulation or repression of this tone from the basal level and its activation still remain to be determined but could be regulated by salt or osmolarity.

In summary, the data in the present study describes evidence for an inhibitory effect of cannabinoidimetics on the Na^+-K^+-ATPase activity of TAL cells. A negative and reciprocal inhibitory interaction between cannabinoids and Ou was evident. Although Ou is a prototypical direct-binding inhibitor of Na^+-K^+-ATPase, the mechanism of cannabinoids had distinct characteristics. A CBR-dependent indirect mechanism is suggested, possibly by G protein–dependent kinase-mediated phosphorylation of Na^+-K^+-ATPase or by alteration of ATP levels in TALs. Further experiments are underway to delineate between these possibilities. The action of AEA to inhibit Na^+ reabsorption by TAL tubules suggests a role for AEA as a modulator of salt-sensitive hypertension.

Authorship Contributions

Participated in research design: Ritter, Ahmad, N. Li, P.-L. Li, Lyall.

Conducted experiments: Ritter, Ahmad, Mummalaneni, Daneva, Dempsey.

Performed data analysis: Ritter, Ahmad, Lyall.

Wrote or contributed to writing of the manuscript: Ritter, Ahmad, N. Li, P.-L. Li, Lyall.

References

Ahmad A, Daneva Z, Li G, Dempsey SK, Li N, Poklis JL, Lichtman A, Li PL, and Ritter JK (2017) Stimulation of diuresis and natriuresis by renomedullary infusion of a dual inhibitor of fatty acid amide hydrolase and monoacylglycerol lipase. *Am J Physiol Renal Physiol* **313**:F1068–F1076.

Ahmad A, Dempsey SK, Daneva Z, Li N, Poklis JL, Li PL, and Ritter JK (2018) Modulation of mean arterial pressure and diuresis by renomedullary infusion of a selective inhibitor of fatty acid amide hydrolase. *Am J Physiol Renal Physiol* **315**: F967–F976.

Askari A (2019) The sodium pump and digitalis drugs: dogmas and fallacies. *Pharmacol Res Perspect* **7**:e00505.

Benowitz NL and Jones RT (1975) Cardiovascular effects of prolonged delta-9-tetrahydrocannabinol ingestion. *Clin Pharmacol Ther* **18**:287–297.

Brailoiu GC, Oprea TI, Zhao P, Abood ME, and Brailoiu E (2011) Intracellular cannabinoid type 1 (CB1) receptors are activated by anandamide. *J Biol Chem* **286**: 29166–29174.

Bénard G, Massa F, Puente N, Lourenço J, Bellocchio L, Soria-Gómez E, Matias I, Delamarre A, Metna-Laurent M, Cannich A, et al. (2012) Mitochondrial CB_1 receptors regulate neuronal energy metabolism. *Nat Neurosci* **15**:558–564.

Carroll MA, McGiff JC, and Ferreri NR (2003) Products of arachidonic acid metabolism. *Methods Mol Med* **86**:385–397.

Chopda GR, Vemuri VK, Sharma R, Thakur GA, Makriyannis A, and Paronis CA (2013) Diuretic effects of cannabinoid agonists in mice. *Eur J Pharmacol* **721**: 64–69.

Deutsch DG, Goligorsky MS, Schmid PC, Krebsbach RJ, Schmid HH, Das SK, Dey SK, Arreaza G, Thorup C, Stefano G, et al. (1997) Production and physiological

actions of anandamide in the vasculature of the rat kidney. *J Clin Invest* **100**: 1538–1546.
Drori A, Permyakova A, Hadar R, Udi S, Nemirovski A, and Tam J (2019) Cannabinoid-1 receptor regulates mitochondrial dynamics and function in renal proximal tubular cells. *Diabetes Obes Metab* **21**:146–159.
Howlett AC and Abood ME (2017) CB_1 and CB_2 receptor pharmacology. *Adv Pharmacol* **80**:169–206.
Hsieh C, Brown S, Derleth C, and Mackie K (1999) Internalization and recycling of the CB1 cannabinoid receptor. *J Neurochem* **73**:493–501.
Lake KD, Compton DR, Varga K, Martin BR, and Kunos G (1997) Cannabinoid-induced hypotension and bradycardia in rats mediated by CB1-like cannabinoid receptors. *J Pharmacol Exp Ther* **281**:1030–1037.
Leterrier C, Bonnard D, Carrel D, Rossier J, and Lenkei Z (2004) Constitutive endocytic cycle of the CB1 cannabinoid receptor. *J Biol Chem* **279**:36013–36021.
Little PJ, Compton DR, Johnson MR, Melvin LS, and Martin BR (1988) Pharmacology and stereoselectivity of structurally novel cannabinoids in mice. *J Pharmacol Exp Ther* **247**:1046–1051.
Loreaux EL, Kaul B, Lorenz JN, and Lingrel JB (2008) Ouabain-Sensitive alpha1 Na,K-ATPase enhances natriuretic response to saline load. *J Am Soc Nephrol* **19**:1947–1954.
Park F, Potukuchi PK, Moradi H, and Kovesdy CP (2017) Cannabinoids and the kidney: effects in health and disease. *Am J Physiol Renal Physiol* **313**:F1124–F1132.
Paronis CA, Thakur GA, Bajaj S, Nikas SP, Vemuri VK, Makriyannis A, and Bergman J (2013) Diuretic effects of cannabinoids. *J Pharmacol Exp Ther* **344**:8–14.
Pertwee RG (1999) Pharmacology of cannabinoid receptor ligands. *Curr Med Chem* **6**: 635–664.
Ritter JK, Li C, Xia M, Poklis JL, Lichtman AH, Abdullah RA, Dewey WL, and Li PL (2012) Production and actions of the anandamide metabolite prostamide E2 in the renal medulla. *J Pharmacol Exp Ther* **342**:770–779.
Rozenfeld R (2011) Type I cannabinoid receptor trafficking: all roads lead to lysosome. *Traffic* **12**:12–18.
Sampaio LS, Taveira Da Silva R, Lima D, Sampaio CL, Iannotti FA, Mazzarella E, Di Marzo V, Vieyra A, Reis RA, and Einicker-Lamas M (2015) The endocannabinoid system in renal cells: regulation of Na(+) transport by CB1 receptors through distinct cell signalling pathways. *Br J Pharmacol* **172**:4615–4625.
Silva GB, Atchison DK, Juncos LI, and García NH (2013) Anandamide inhibits transport-related oxygen consumption in the loop of Henle by activating CB1 receptors. *Am J Physiol Renal Physiol* **304**:F376–F381.
Sofia RD, Knobloch LC, Harakal JJ, and Erikson DJ (1977) Comparative diuretic activity of delta9-tetrahydrocannabinol, cannabidiol, cannabinol and hydrochlorothiazide in the rat. *Arch Int Pharmacodyn Ther* **225**:77–87.
Vollmer RR, Cavero I, Ertel RJ, Solomon TA, and Buckley JP (1974) Role of the central autonomic nervous system in the hypotension and bradycardia induced by (-)-delta 9-trans-tetrahydrocannabinol. *J Pharm Pharmacol* **26**: 186–192.
Wise LE, Iredale PA, Stokes RJ, and Lichtman AH (2007) Combination of rimonabant and donepezil prolongs spatial memory duration. *Neuropsychopharmacology* **32**:1805–1812.
Yu M, Lopez B, Dos Santos EA, Falck JR, and Roman RJ (2007) Effects of 20-HETE on Na+ transport and Na+ -K+ -ATPase activity in the thick ascending loop of Henle. *Am J Physiol Regul Integr Comp Physiol*, **292**:R2400–R2405.

Address correspondence to: Joseph K. Ritter, Department of Pharmacology and Toxicology, Virginia Commonwealth University, Box 980613, Richmond, VA 23298-0613. E-mail: jritter@vcu.edu, 828-0676

MS #JPET-AR-2020-000163

Supplementary Figures

Mechanism of diuresis and natriuresis by cannabinoids: evidence for inhibition of Na^+-K^+-ATPase in mouse kidney thick ascending limb tubules

Joseph K. Ritter, Ashfaq Ahmad, Shoba Mummalaneni, Zdravka Daneva, Sara K. Dempsey, , Ningjun Li, Pin-Lan Li, and Vijay Lyall

SFig. 1. Effect of bumetanide (Bu) and CP55940 (CP) on Na^+ influx in mTAL cells induced by changes in bath Na^+. (A) A mTAL tubule from WT mouse was loaded with SBFI and was initially perfused with 0 Na R (pH 7.4) containing 140 mM NMDG-Cl. In the first step, 0 Na R was replaced with the CR (pH 7.4) containing 140 mM NaCl. After the FIR reached a plateau, the solution was changed back to 0 Na R. In the second step, 0 Na R was replaced with CR + 50 uM Bu. The tissue was then placed in 0 Na R for 10 min to achieve its baseline value. In the third step, 0 Na R was replaced with CR + 10 μM CP. After the FIR reached a plateau, the solution was changed to 0 Na R + CP and then to 0 Na R in a stepwise manner. The changes in Na^+ flux was measured as temporal changes in FIR (F_{340}/F_{380}). The mean ± SEM FIR values were calculated from 33 regions of interest (ROIs). Vertical bars represent the time periods when different solutions were switched during the experiment. **(B)** Shows the mean maximum changes in FIR (max) and the initial slope (ΔFIR/min) in response to changes in external Na^+ from 0 to 140 mM, in the absence and presence of 50 μM Bu. *p = 0.0001 (n = 33).

SFig. 2. Effect of oubain (Ou) and bumetanide (Bu) on $[Na^+]_i$ in mTAL cells. A mTAL tubule from WT mouse was loaded with SBFI and was initially perfused with CR (pH 7.4).

The CR was first changed to CR + 2 mM Ou. After the FIR reached a plateau, the solution was changes to CR + Ou + 100 μM Bu. The Changes in steady-state $[Na^+]_i$ were measured as temporal changes in FIR (F_{340}/F_{380}). The mean ± SEM FIR values were calculated from 18 regions of interest (ROIs). Vertical bars represent the time periods when different solutions were switched during the experiment.

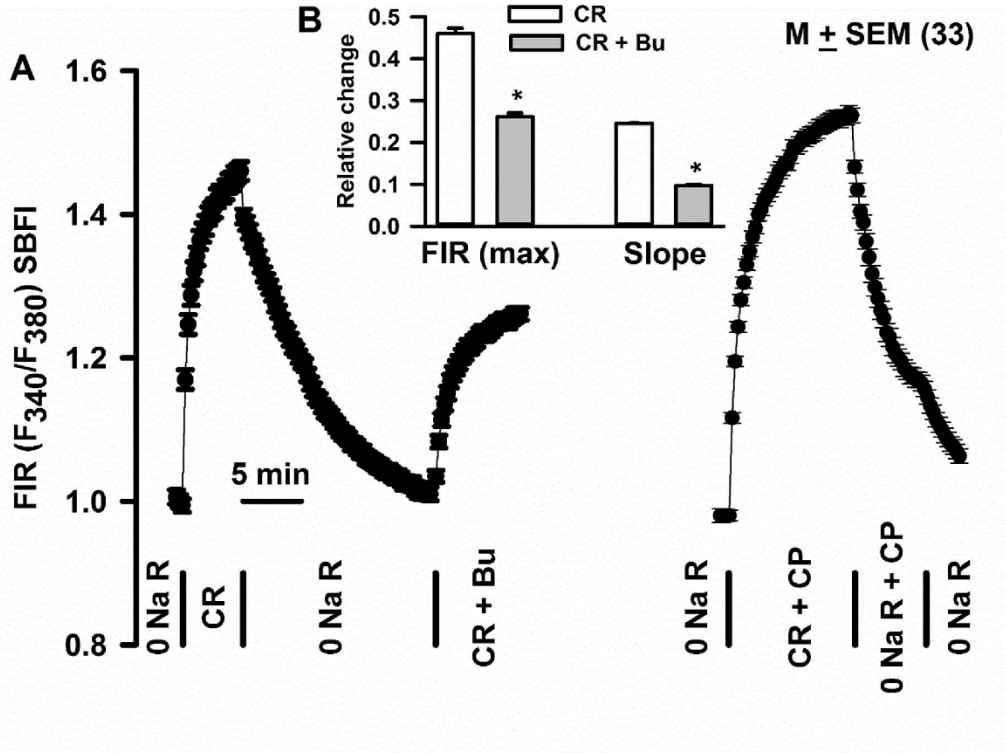

sFig. 1. Effect of bumetanide (Bu) and CP55940 (CP) on Na^+ influx in mTAL cells induced by changes in bath Na^+

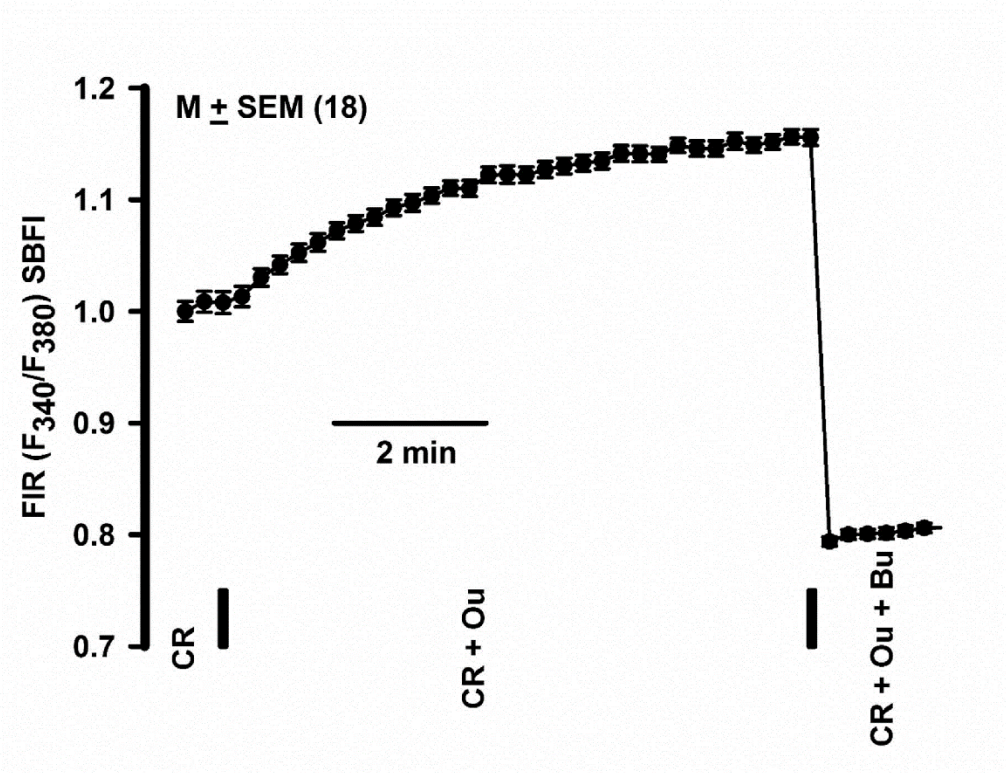

SFig. 2. Effect of oubain (Ou) and bumetanide (Bu) on $[Na^+]_i$ in mTAL cells